Electronic structure and magnetic and hyperfine properties of dilute alloys of Fe in Ti and Zr hosts

D. E. Ellis

Department of Physics and Astronomy, Northwestern University, Evanston, Illinois 60201

Diana Guenzburger

Argonne National Laboratory, 9700 South Cass Ave., Argonne, Illinois 60439
and Department of Physics and Astronomy, Northwestern University, Evanston, Illinois 60201

(Received 4 June 1984)

The electronic structure of clusters containing 15 atoms which represent substitutionally disordered Fe Ti alloys is obtained with the discrete variational method and the local $X\alpha$ approximation to the exchange interaction. Local magnetic moments and isomer shift values are derived, and their variation with local lattice compression calculated. Similar studies are done for ternary bcc β-TiZr(Fe) alloys, and existing Mössbauer data interpreted with our theoretical results.

I. INTRODUCTION

A nonmagnetic transition-metal host may form solid solutions in which some atoms in the lattice sites are randomly substituted for by a magnetic impurity. In such cases, many questions arise as to local electronic properties at the impurity site, as well as perturbations caused on the host, and these have been the subject of much experimental and theoretical investigation. Among the experimental techniques well suited to the study of local properties is Mössbauer spectroscopy, which allows measurements of hyperfine interactions between the probe nucleus and its electronic environment. The most convenient Mössbauer probe is ^{57}Fe, and thus this technique has been widely employed to study Fe alloys in the dilute or concentrated limits.

The solubility of Fe in β-Ti (bcc structure) can be extended to as much as 35 at. %, by the use of a "splat-quenching" technique,[1,2] forming a phase in which Fe substitutes randomly for the Ti atoms of the host. X-ray diffraction studies, although they can give information on the changes in the average lattice parameter with the concentration of the solute,[1,2] do not show, however, whether any local order is present, or whether local distortions around the solute atoms exist. Mössbauer hyperfine interactions may give some clues to answer such questions, and reports have been given of extensive studies of Mössbauer spectroscopy of β-Ti(Fe) alloys at several concentrations,[2–7] in which isomer shifts (I_S) and quadrupole splittings (ΔE_Q) were measured.

Since such hyperfine interactions are related to the electronic environment of an Fe atom, electronic structure calculations of the I_S and ΔE_Q would be valuable to extract what information these parameters can give. The work described in this paper is aimed at investigating the electronic and magnetic properties of dilute Fe solutions in β-Ti and related alloys. I_S and ΔE_Q values are calculated and related to the electronic and structural properties.

The theoretical approach that we have used for this problem is to calculate the electronic structure of 15-atom clusters that represent the alloys, using the first-principles self-consistent discrete variational method. Complete band-structure calculations of dilute alloys are extremely time consuming because of the large number of atoms to be included in the unit cell; on the other hand, the cluster model has been used lately in several cases, with very promising results, to study the properties of metals and alloys.[8–11]

In a previous paper[12] we have reported results of cluster calculations for Fe metal, Ti Fe alloys, and the intermetallic compound TiFe. We have successfully predicted the ferromagnetic coupling in Fe and the antiferromagnetically coupled moment which is observed in dilute Ti impurities in Fe. The I_S of Fe at different lattice constants correlated very well with the experimentally observed dependence with pressure, and the calculated I_S in TiFe compares very well with the measured value.

In view of these encouraging results and of the wealth of data on β-Ti(Fe), we have extended our calculations to these alloys. Since quadrupole splittings are observed, we have calculated ΔE_Q values for clusters representing alloys in which a field gradient would occur. To our knowledge, this is the first report of calculations on field gradients due to impurities in metals, within a first-principles cluster model.

Ternary alloys of the type β-TiZr(Fe) were investigated by Mössbauer spectroscopy, since it was discovered that the addition of Ti was necessary to retain the β-Zr(Fe) phase by quenching.[13] The physical problem posed by the substitution of a $3d$ transition element atom by a $4d$ atom in the binary alloy β-Ti(Fe) attracted our attention, and so we have extended our calculations to cluster models for this case.

II. THEORETICAL METHOD

A. Electronic structure calculations

In Fig. 1 we show the cluster containing 15 atoms which was chosen to represent the alloys with bcc structure. The electronic structure calculations were performed with the first-principles discrete variational method (DVM), which has been described in detail elsewhere.[14,15] The local $X\alpha$ approximation for the exchange interaction was employed.[16] We have used the DVM method in our previously reported calculations[12] on Fe and TiFe alloys, and here we follow the same general procedure.

The basic problem is to solve self-consistently the one-electron eigenvalue equations, in which the Hamiltonian is a functional of the electronic density at some point $\vec{r}$. The exchange potential is given by (in Hartree units)

$$V_{X\alpha}(\rho_\sigma) = -3\alpha \left[\frac{3\rho_\sigma(\vec{r})}{4\pi} \right]^{1/3} \tag{1}$$

and the value $\alpha = \frac{2}{3}$ was employed.[16] The Coulomb potential in the Hamiltonian includes nuclear and electronic components, and the density is constructed as a sum over the molecular spin orbitals $\phi_{j\sigma}$ with occupation $n_{j\sigma}$:

$$\rho_\sigma(\vec{r}) = \sum_j n_{j\sigma} |\phi_{j\sigma}(\vec{r})|^2 . \tag{2}$$

Different densities at point $\vec{r}$ for different spins may be obtained by allowing the spacial orbitals $\phi_{j\uparrow}$ and $\phi_{j\downarrow}$ to have different shapes for different spins, in addition to the contributions of unpaired spins.

The actual electron charge density is replaced by a model density $\rho_{scc}(\vec{r})$, which is a superposition of radial densities centered on the cluster atoms ν, weighted by the Mulliken[17] populations P_{nl}^ν of the orbitals:[15]

$$\rho_{scc}(\vec{r}) = \sum_{\nu,n,l} P_{nl}^\nu |R_{nl}^\nu(r_\nu)|^2 . \tag{3}$$

The model potential derived from this density is expected to be well suited for compact structures such as are present in metals; for directional bonds or general cases of highly anisotropic charge distributions, a more exact fit to the molecular charge density, obtained through a multipolar expansion of $\rho(\vec{r})$, is necessary for more precise results.[18]

The molecular spin orbitals $\phi_{i\sigma}$ are expanded on a basis of numerical atomic orbitals [linear combination of atomic orbitals (LCAO) approximation]. We have used spherical potential wells around the atoms to obtain more contracted valence orbitals, which include $3d$, $4s$, and $4p$ for Fe and Ti, and $4d$, $5s$, and $5p$ for Zr. One finally solves the usual secular equations self-consistently. The matrix elements of the Hamiltonian and overlap matrices are obtained by numerical integration. In the usual DVM, a random integration method ("diophantine")[14] is employed; however, in the case of hyperfine interactions, the calculations require much greater caution in the numerical procedures, especially at the core region of the probe atom, where precision of matrix elements for the rapidly varying functions is difficult to achieve. Thus a special
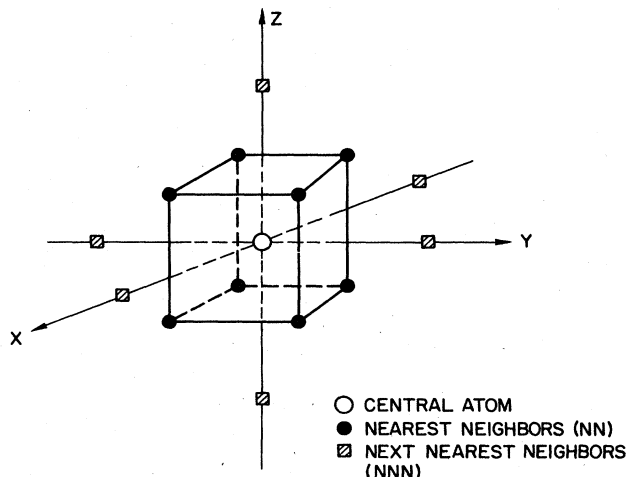
FIG. 1. Cluster of 15 atoms representing bcc alloys.

○ CENTRAL ATOM
● NEAREST NEIGHBORS (NN)
▨ NEXT NEAREST NEIGHBORS (NNN)

integration scheme has been derived, and used within a sphere of radius ~ 2 a.u. involving a systematic polynomial integration in three dimensions.[12,19]

The 15-atom cluster is embedded in the solid by considering numerical atomic potentials at a number of sites surrounding the cluster. These potentials are truncated to simulate orthogonality effects.[10]

B. Mössbauer isomer shifts and quadrupole splittings

The isomer shift of an absorber A relative to a source S in a Mössbauer spectroscopy measurement is given by[20]

$$I_S = \frac{2\pi}{3} Ze^2 (\Delta\langle r^2\rangle) S'(Z)[\rho(0)_A - \rho(0)_S] \tag{4}$$

or

$$I_S = \alpha[\rho(0)_A - \rho(0)_S] . \tag{5}$$

α is often referred to as the I_S calibration constant. In Eq. (4), Z is the nuclear charge of the probe atom, $\Delta\langle r^2\rangle$ is the difference of the mean-square nuclear radius between the excited and ground states of the nuclear Mössbauer transition (14.4 keV for ^{57}Fe), and $S'(Z)$ is a correction for relativistic effects.

In the single-particle approximation, the total electronic density at a nucleus is given by the sum of $\rho_\uparrow(0)$ and $\rho_\downarrow(0)$, as defined in Eq. (2). Only the molecular orbitals belonging to the totally symmetric representation will have amplitude different from zero at the origin.

As explained in Ref. 12, we have neglected the $1s$ and $2s$ contributions, since differences in $\rho(0)$ for these orbitals in different environments are negligible.

The quadrupole splitting ΔE_Q of the $I = \frac{3}{2}$ excited state of ^{57}Fe of the 14.4-keV transition is given by[20]

$$\Delta E_Q = \frac{1}{2} eQV_{zz} \tag{6}$$

for the case of axial symmetry. The field gradient V_{zz} has contributions from the electrons and the other nuclei surrounding the probe nucleus. In the orbital approximation:

$$V_{zz} = \sum_k Z_k \frac{3z_k^2 - r_k^2}{r_k^5} - \sum_{i\sigma} n_{i\sigma} \left\langle \phi_{i\sigma} \left| \frac{3z^2 - r^2}{r^5} \right| \phi_{i\sigma} \right\rangle . \tag{7}$$

The electronic matrix elements require careful evaluation, since the final value results from a delicate balance between positive and negative terms. Once the molecular spin orbitals $\phi_{i\sigma}$ are expanded on the LCAO basis, one-, two-, and three-center integrals over atomic orbitals appear. The one-center terms are straightforward, since they are the product of the eigenvector coefficients and the atomic $\langle r^{-3} \rangle$ integral. The two- and three-center integrals require special integration methods described elsewhere.[21,22]

III. RESULTS AND DISCUSSION

A. Fe as a dilute impurity in the Ti host

In Table I we show results relative to the case of a very dilute solution of Fe in bcc Ti metal, represented by a cluster such as depicted in Fig. 1, in which the central atom is Fe and all others are Ti. The clusters are embedded in a Ti lattice. Results for Fe_{15}, which have been previously reported,[12] are repeated here for the sake of comparison.

The lattice parameter of β-Ti is 3.29 Å, as extrapolated to room temperature,[1,2] and this would be representative of the dilute limit, if no local distortions were present. The results for this case show that a large moment on Fe is retained, larger than in Fe metal, and a small moment is induced in the surrounding Ti atoms, coupled antiferromagnetically to the Fe. The moments in Table I, as for

all cases presented further on, were calculated as the difference in the Mulliken population[17] for spin ↑ and spin ↓ electrons ($3d$, $4s$, and $4p$). For this β-Ti interatomic distance, the Fe atom's moment is almost unaffected by the metal in which it is embedded, having a somewhat similar behavior to a Van Vleck ionic moment.

We have also done self-consistent calculations decreasing uniformly the lattice parameter for the cluster atoms and surrounding atomic potentials, representing in a simple way a local compression around the Fe atom. A dramatic effect on the moment is observed, which decreases and finally collapses to zero. Mössbauer spectroscopy studies in the presence of a magnetic field seem to indicate a zero or very small magnetic moment on Fe in dilute β-Ti(Fe).[7] Thus the results of our calculations suggest that a lattice compression around the impurity takes place. Indeed, recent experiments with extended x-ray absorption fine structure (EXAFS) spectroscopy[23] make possible the observation of local distortions around impurity atoms in metals, and the few cases reported show a shortening of the nearest-neighbor (NN) distance around a smaller impurity atom when it is substituting a metal atom with a larger atomic radius. The largest distortion observed so far with EXAFS was about −0.13 Å, for Cu impurities in Al. We cannot make an exact prediction of the distortion which would actually suppress the Fe moment entirely, for two reasons. First, we have modeled the compression around the impurity by decreasing uniformly all interatomic distances, when actually the NN

TABLE I. Magnetic moments and isomer shifts calculated at the central Fe atom in Fe_{15}, $FeTi_{14}$, and $FeTi_8Fe_6$ clusters.

Cluster	Lattice parameter (Å)	$\mu(Fe_c)$ (μ_B)	$\mu(NN)$ (μ_B)	$\rho(0)$ (a_0^{-3})		I_S (calc.) (mm/s)	I_S (expt.) (mm/s)
Fe_{15}[a]	2.866	2.80	3.39	$3s$ valence	139.93 <u>6.53</u> 146.46	0	0
$FeTi_{14}$	3.29[b]	3.52	−0.69	$3s$ valence	140.40 <u>5.43</u> 145.83	+ 0.16	
$FeTi_{14}$	3.18	2.98	−0.60	$3s$ valence	140.28 <u>5.88</u> 146.16	+ 0.08	
$FeTi_{14}$	3.06	1.42	−0.32	$3s$ valence	140.16 <u>6.48</u> 146.64	−0.05	−0.24[c]
$FeTi_{14}$	2.866	0.06	−0.01	$3s$ valence	140.00 <u>7.73</u> 147.73	−0.32	
$FeTi_8Fe_6$[a] (CsCl)	2.95	2.09	−1.58	$3s$ valence	140.01 <u>7.04</u> 147.05	−0.148	−0.145[d]

[a]Results from Ref. 12.
[b]Equilibrium lattice parameter of β-Ti; see Refs. 1 and 2.
[c]From Refs. 2 and 5.
[d]From Ref. 26.

distance will be more affected, the next-nearest-neighbor (NNN) distance less, and so on. The second reason refers to our study of the pressure effect on the magnetic moment of Fe metal,[12] a clear-cut case in which our theoretical results could be compared directly to experimental measurements. We found that our 15-atom cluster calculations give moments somewhat higher than those found experimentally, and although we obtained the right trend for the behavior of μ_{Fe} with the shortening of the lattice parameter, the calculated moments showed a decrease which was less pronounced than what is actually observed.

We may compare this case of a Fe impurity in the nonmagnetic Ti metal to the inverse case which we have previously studied,[12] that is, a Ti impurity in Fe metal. The latter calculations show a large moment on Ti, which is observed experimentally by neutron scattering. It is driven by the magnetic lattice and is coupled antiferromagnetically to it. In the present case, the results show that the Fe atom will preserve its moment in the Ti nonmagnetic lattice if it is sufficiently isolated. However, any reduction in impurity-neighbor distance will have a strong effect towards suppressing the moment. The recently reported EXAFS measurements of NN distances of impurities tend to support the hypothesis of a contraction, reducing or suppressing the magnetic moment on the Fe atom, since its atomic radius (1.26 Å) is considerably smaller than Ti (1.47 Å).

Figures 2 and 3 show the local density of states (DOS) diagram for Fe in FeTi$_{14}$, at lattice parameters 3.29 and 2.87 Å. These diagrams have the spin ↑ and spin ↓ DOS normalized to constant peak height, and are obtained by broadening the discrete energy levels of the cluster by Lorentzians, to simulate a continuum. Once again, the disappearance of the magnetic moment on Fe with lattice compression is made clear.

We now comment on the values of the I_S at the Fe atom, relative to Fe metal. The measured value extrapolated to the dilute limit is approximately -0.24 mm/sec relative to Fe metal.[2,5] We observe that the theoretical value at 3.29 Å is not compatible with the experimental value, indeed it has even the wrong sign. The I_S values were calculated using Eq. (5), with $\alpha = -0.25a_0^3$ (mm/s), the value derived from our previous calculations for Fe metal at different pressures,[12] and which also agrees with the best estimates previously reported.[24,25] As the lattice parameter is shortened, the I_S values decrease and become negative, through the increase of the valence contribution. The valence contribution is augmented at shorter distances due to the so-called "overlap distortion,"[20] which means that the orbitals of a_1 symmetry distort towards the nucleus since they have to be orthogonal to the core orbitals of the neighbors. Charge transfer from the Ti neighbors into the Fe valence orbitals also takes place, as can be expected due to the difference in the Pauling electronegativities (1.8 for Fe, 1.5 for Ti). However, we have found that it does not change much with the interatomic distance. For the four cases in Table I we find an average value of 0.28 ± 0.07 transferred electrons, as calculated with Mulliken populations.

Since our previous investigation on Fe metal and TiFe alloys gave excellent results regarding the I_S, we are more confident to suggest that, to match the experimental number, a large compression around the Fe atom must take place; more precisely the NN distance to the Fe atom would have to decrease by 0.31 Å (lattice parameter for the cluster$=2.93$ Å). This prediction is somewhat handi-
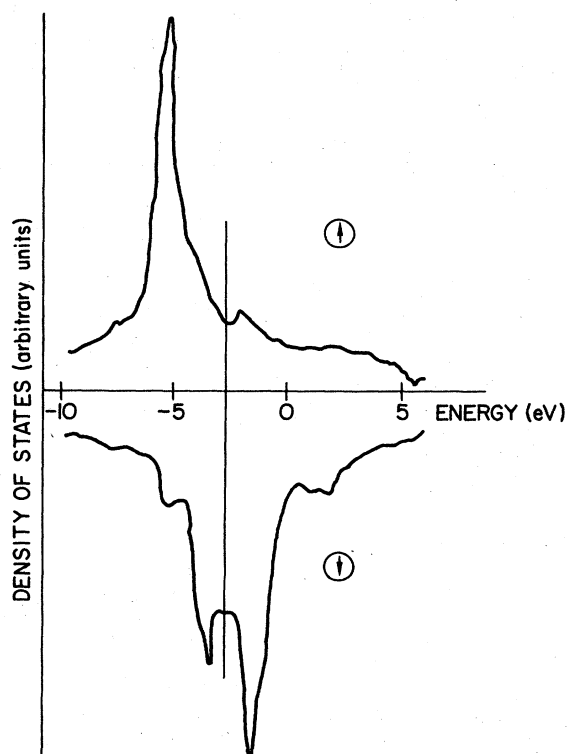
FIG. 2. Local density of states (including $3d$, $4s$, and $4p$ components) of the central Fe atom in the FeTi$_{14}$ cluster, at lattice parameter $a=3.29$ Å.
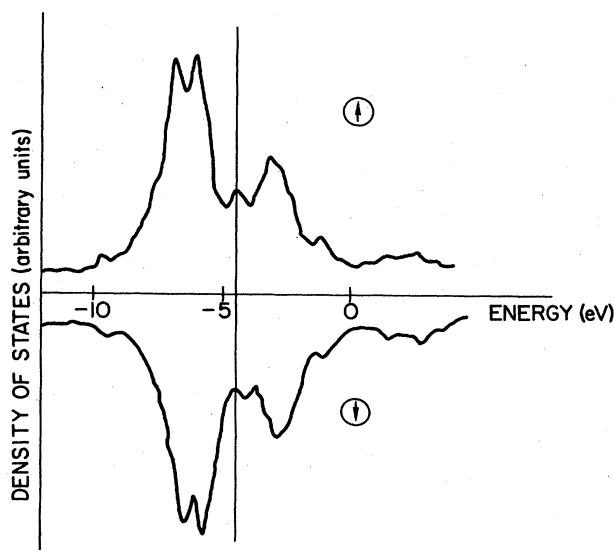
FIG. 3. Local density of states (including $3d$, $4s$, and $4p$ components) of the central Fe atom in the FeTi$_{14}$ cluster, at lattice parameter $a=2.87$ Å.

TABLE II. Magnetic moments, isomer shifts, and quadrupole splittings of Fe(FeTi₇)Ti₆ clusters, embedded in Ti metal, calculated at the central Fe atom.

Cluster	Lattice parameter (Å)	$\mu(Fe_c)$ (μ_B)	$\rho(0)$ (a_0^{-3})	I_S[a] (calc.) (mm/s)	I_S[b] (expt.) (mm/s)	EFG[c] (a_0^{-3})		ΔE_Q[d] (calc.) (mm/s)	ΔE_Q[e] (expt.) (mm/s)
FeTi₁₄	3.29	3.52	3s 140.40 / valence 5.43 / 145.83	+0.16	−0.24	—		—	—
Fe(FeTi₇)Ti₆ (C₃ᵥ)	3.29	3.49	3s 140.55 / valence 5.30 / 145.85	+0.15		N	+0.1538	+0.29	
						$1c\uparrow$	−0.0112		
						Total↑	−0.1115		
						$1c\downarrow$	+0.1675		
						Total↓	+0.1412		
Fe(FeTi₇)Ti₆	3.13	2.18	3s 140.38 / valence 6.00 / 146.38	+0.02	−0.16 to −0.24 (dilute limit)	N	+0.1793	+0.32	~0.20
						$1c\uparrow$	−0.0137		
						Total↑	−0.1232		
						$1c\downarrow$	+0.1719		
						Total↓	+0.1473		
Fe(FeTi₇)Ti₆ (lattice d_e)	3.13	1.99	3s 140.27 / valence 6.12 / 146.39	+0.02		N	+0.1793	+0.37	
						$1c\uparrow$	+0.0090		
						Total↑	−0.0995		
						$1c\downarrow$	+0.1815		
						Total↓	+0.1561		
Fe(FeTi₇)Ti₆ (lattice d_e)	2.96	0.16	3s 140.05 / valence 7.17 / 147.22	−0.19		N	+0.2109	+0.59	
						$1c\uparrow$	+0.1791		
						Total↑	+0.0565		
						$1c\downarrow$	+0.1409		
						Total↓	+0.1085		

[a] $I_S = -0.25\Delta\rho(0)$.

[b] From Refs. 2 and 5.

[c] Field gradients (V_{zz}) as defined in Eq. (7). "N" is the nuclear contribution of surrounding atoms in the cluster $[\sum_k Z_k(3z_k^2 - r_k^2)/r_k^5]$, partially cancelled by the core electrons. In our calculations, the $1s$, $2s$, and $2p$ orbitals of Fe, and the $1s$, $2s$, $2p$, $3s$, and $3p$ orbitals of Ti were considered as core orbitals, orthogonalized to the valence orbitals which are included in the variational calculation. The total electronic contributions are defined as $-\sum_{i\sigma} n_{i\sigma}\langle\phi_{i\sigma}|(3z^2-r^2)/r^5|\phi_{i\sigma}\rangle$; "$1c$" stands for the one-center part of this last term, and the arrows refer to the spin.

[d] Quadrupole moment of the ⁵⁷Fe excited state taken as 0.156 b [see N. Ray and T. P. Das, Phys. Rev. B 16, 4794 (1977)].

[e] See Refs. 2 and 6.

TABLE III. Magnetic moments, isomer shifts, and quadrupole splittings of $Fe(Ti)_8Fe_xTi_{6-x}$ clusters, embedded in Ti metal, calculated at the central Fe atom.

Cluster	Lattice parameter (Å)	$\mu(Fe_c)$ (μ_B)	$\rho(0)$ (a_0^{-3})	I_S^a (calc.) (mm/s)	I_S^b (expt.) (mm/s)	EFG[c] (a_0^{-3})	ΔE_Q^d (calc.) (mm/s)	ΔE_Q^e (expt.) (mm/s)
$FeTi_{14}$ (O_h)	3.29	3.52	3s 140.40 valence 5.43 145.83	+0.16	−0.24	—	—	—
$Fe(Ti)_8FeTi_5$ (C_{4v})	3.29	3.54	3s 140.36 valence 5.42 145.78	+0.17		N +0.0999 $1c\uparrow$ −0.0161 Total↑ −0.0830 $1c\downarrow$ +0.0224 Total↓ −0.0054	+0.02	
$Fe(Ti)_8FeTi_5$ (C_{4v})	2.96	0.98	3s 140.12 valence 6.98 147.10	−0.16	−0.16 to −0.24	N +0.1371 $1c\uparrow$ +0.0235 Total↑ −0.0575 $1c\downarrow$ +0.0546 Total↓ +0.0017	+0.13	~0.20
$Fe(Ti)_8Fe_3Ti_3^f$ (C_{3v})	3.29	3.66	3s 140.47 valence 5.58 146.05	+0.10		N 0.0 $1c\uparrow$ −0.1978 Total↑ −0.1804 $1c\downarrow$ +0.0178 Total↓ +0.0342	−0.23	
$Fe(Ti)_8Fe_4Ti_2^g$ (D_{4h})	3.05	2.17	3s 140.24 valence 6.45 146.69	−0.06		N −0.2507 $1c\uparrow$ −0.0243 Total↑ +0.1236 $1c\downarrow$ +0.0643 Total↓ +0.1211	−0.01	

[a] $I_S = -0.25\Delta\rho(0)$.
[b] From Refs. 2 and 5.
[c] See references for Table II.
[d] Quadrupole moment of the ^{57}Fe excited state taken as 0.156 b.
[e] See Refs. 2 and 6.
[f] Three Fe NNN atoms at positive x,y,z coordinates.
[g] Four Fe NNN atoms on equatorial plane.

TABLE IV. Contributions to the field gradient V_{zz} on the central Fe for Fe-Ti clusters (in a.u.).

Cluster	Lattice parameter (Å)	Nuclear[a] (core electrons subtracted)	Total spin↑	Total spin↓	Total one center (↑+↓)	Total two and three center (↑+↓)
Fe(FeTi$_7$)Ti$_6$	3.29	+0.154	−0.112	+0.141	+0.156	−0.127
Fe(FeTi$_7$)Ti$_6$	3.13	+0.179	−0.123	+0.147	+0.158	−0.134
Fe(FeTi$_7$)Ti$_6$	2.96 (lattice d_e)	+0.211	+0.057	+0.109	+0.320	−0.155
Fe(Ti)$_8$FeTi$_5$	3.29	+0.100	−0.083	−0.005	+0.006	−0.095
Fe(Ti)$_8$FeTi$_5$	2.96	+0.137	−0.058	+0.002	+0.078	−0.134
Fe(Ti)$_8$Fe$_3$Ti$_3$[b]	3.29	0.0	−0.180	+0.034	−0.180	+0.034
Fe(Ti)$_8$Fe$_4$Ti$_2$[b]	3.05	−0.251	+0.124	+0.121	+0.040	+0.205

[a]See Ref. c of Table II.
[b]See Refs. f and g of Table III.

capped by the simple model of uniform compression, as mentioned before, but it is compatible with both the I_S and the magnetic moment.

The last entry in Table I (FeTi$_8$Fe$_6$) is for results of calculations reported in Ref. 12 for the 50-50 at. % compound TiFe (CsCl structure), and is shown for comparison with the dilute FeTi case. Since for this dilute impurity we have predicted an interatomic distance around the impurity approximately of the same order as in the TiFe compound, the higher $\rho(0)$ and lower I_S for the impurity at the same lattice parameter is consistent with the higher charge transfer, into the Fe valence orbitals, from the many shells of Ti atoms surrounding the impurity.

B. β-Ti(Fe) at higher concentrations

The bcc phase β-Ti(Fe) with substitutional disorder is retained at room temperature by quenching techniques, at concentrations ranging from 0 to 22 at. % Fe.[1,2] I_S and ΔE_Q values have been measured in this range of concentrations.[2,6] The ΔE_Q shows a surprising behavior, since it almost does not vary with concentration, having a value around 0.2 mm/s,[2] and also does not vary with the techniques used in the preparation of the sample.[6] The I_S is lower than for the compound TiFe, having a value around −0.16 mm/s for concentrations between ∼12 and 22 at. % Fe, and decreasing further for more dilute cases.[2,5] A value around −0.24 mm/s may be extrapolated in the dilute limit.

A mechanism has been proposed in which a locally ordered solid solution is obtained in β-Ti(Fe), in which the Fe atoms attract Ti atoms preferably, so that eventually each Fe atom is entirely surrounded by Ti first neighbors.[2,5] This local order, among other considerations, was proposed on the basis of a stronger force constant derived for Fe-Ti pairs, compared to Ti-Ti.[4]

In this work we have tried to reproduce with our clusters some situations that may occur when the Fe concentration is increased, so that some general effects may be derived. These may be divided in two main categories, that is, Fe atoms forming clusters with the central atom, by substituting one or more Ti first neighbors, or Fe atoms substituting only Ti second neighbors. It is clear, however, that a large number of possible types of clustering and even lattice distortions may occur in such a complex substitutionally disordered solid solution, and we do not attempt to solve the problem in its whole complexity. For all these calculations the clusters are embedded in the Ti lattice.

In Table II we give results for the cases studied of the Fe(FeTi$_7$)Ti$_6$ clusters, in which one first-neighbor Ti atom has been substituted for Fe. The results show that one Fe next neighbor does not have much influence on the I_S at the central Fe, especially at distances of the order of the Ti lattice distance. The ΔE_Q is positive (+ 0.29 mm/s) at the Ti lattice parameter 3.29 Å, and increases for compressed distances.

We point out, however, that the precision with which we can derive the I_S, which is quite high as seen in Ref. 12, is not matched by the ΔE_Q calculations. In the latter case we have observed that, as the symmetry is lowered to

TABLE V. Magnetic moments, isomer shifts, and quadrupole splittings of clusters representing Fe-Zr and Fe-Zr-Ti alloys.

Cluster	Lattice parameter (Å)	$\mu(Fe_c)$ (μ_B)	$\rho(0)$ (a_0^{-3})	I_S^b (calc.) (mm/s)	I_S^c (expt.) (mm/s)	EFG^d (a_0^{-3})	ΔE_Q^e (calc.) (mm/s)	ΔE_Q (expt.) (mm/s)
$FeTi_{14}$	3.29	3.52	3s 140.40 valence 5.43 145.83	+0.16	−0.24	—	—	—
$FeZr_{14}$	3.60[a]	3.78	3s 140.60 valence 4.85 145.45	+0.25	~−0.13	—	—	—
$Fe(ZrTi_7)Ti_6$ (C_{3v}) (embedded in Ti)	3.29	3.46	3s 140.56 valence 5.38 145.94	+0.13		N 0.0 $1c-\uparrow$ +0.0086 Total↑ +0.0087 $1c-\downarrow$ −0.0776 Total↓ −0.0703	−0.10	(see text)
$Fe(Zr_2Ti_6)Ti_6$[f] (embedded in Ti)	3.29	3.37	3s 140.56 valence 5.43 145.99	+0.12	−0.13 to −0.24	N 0.0 $1c-\uparrow$ −0.0010 Total↑ −0.0090 $1c-\downarrow$ −0.1239 Total↓ −0.1154	−0.20	
$Fe(TiZr_7)Zr_6$ (embedded in Zr)	3.60	3.81	3s 140.63 valence 4.80 145.43	+0.26		N 0.0 $1c-\uparrow$ −0.0298 Total↑ −0.0230 $1c-\downarrow$ +0.0596 Total↓ +0.0621	+0.06	

[a] See Ref. 13.
[b] $I_S = -0.25\,\Delta\rho(0)$.
[c] See Refs. 2 and 5.
[d] See references to Table II.
[e] $Q(^{57}Fe) = 0.156$ b.
[f] Two Zr atoms at opposite sites on C_{3v} axis.

TABLE VI. Contributions to the field gradient V_{zz} on the central Fe for Fe-Ti-Zr clusters (in a.u.).

Cluster	Lattice parameter (Å)	Nuclear[a] (core electrons subtracted)	Total↑	Total↓	Total one center (↑+↓)	Total two and three center (↑+↓)
Fe(ZrTi₇)Ti₆	3.29	0.0	+0.009	−0.070	−0.069	+0.007
Fe(Zr₂Ti₆)Ti₆[b]	3.29	0.0	−0.009	−0.115	−0.125	+0.001
Fe(TiZr₇)Zr₆	3.60	0.0	−0.023	+0.062	+0.030	+0.009

[a]See Ref. c of Table II.
[b]Two Zr atoms at opposite sites on C_{3v} axis.

C_{3V}, even for the FeTi₁₄ cluster a spurious field gradient builds up, due to accumulation of numerical errors. We conclude that, although the order of magnitude and the trends of our ΔE_Q are certainly correct, the absolute values may have uncertainties, which we estimate as being as high as ~50% in some cases. So we conclude that to match the experimental I_S values a contraction would have to take place if these configurations are present, and in this case, such type of clustering would produce a positive field gradient. The rather large predicted ΔE_Q 0.4—0.6 mm/s suggests that nearest-neighbor clustering is not very frequent, in agreement with the model of Galvão da Silva.[2,5] Unfortunately, the sign of ΔE_Q has not yet been measured.

The two entries in Table II for lattice parameter 3.13 Å differ by having a uniform lattice parameter in the first case (including the outer atoms of the cluster embedding), and in the second case, maintaining a lattice parameter of 3.29 Å, which corresponds to β-Ti, for the atoms exterior to the cluster. It is seen that the influence of the position of the exterior atoms is small.

As for the magnetic moment on the central Fe atom, comparison with the numbers in Table I shows that no significant changes are induced by the presence of an Fe first neighbor.

In Table III we give results for clusters in which one or more second-neighbor Ti atoms have been substituted by Fe. These clusters are consistent with the hypothesis of local order that has been put forth.[2,5] The values of ΔE_Q obtained are also positive for one Fe NNN, but much smaller than in the case of one Fe NN. For compressed distances, they are more compatible with the experimental value, while at these distances, the Fe NN gives considerably larger field gradients. However, for different arrangements of the Fe NNN atoms, as in the two last entries of Table III, the sign is reversed, so the situation is seen to be very complex. Again, we point out the importance of the experimental determination of the sign of the field gradient.

In Table IV the various contributions to the field gradient are discriminated. For one Fe NN we observe that the total two- and three-center contributions are not much different in absolute value to the nuclear term, and these two combined together largely cancel. This indicates that even the valence electrons on the NN Fe atom are mostly seen by the central Fe as negative point charges. The positive sign of V_{zz} is thus mainly determined by the large one-center positive terms.

In the case of one NNN Fe atom, the one-center contribution is also positive but of much smaller value, resulting in a much smaller total field gradient. Table III also shows, with comparison to Table I, that Fe second neighbors produce very small changes on the I_S of the Fe atom at comparable distances.

C. β-TiZr(Fe) ternary alloys

Although the β-Zr(Fe) solid solution is not retained by quenching, addition of small amounts of Ti stabilizes this phase.[13] This feature has allowed a series of experimental measurements on these substitutionally disordered bcc ter-

nary alloys, using Mössbauer spectroscopy, x-ray diffraction, and scanning electron microscopy.[13] From a theoretician's point of view, the effect of the interchange of Zr ($4d$ element) and Ti ($3d$ element) as hosts in the lattice is interesting inasmuch as Zr, although being in the same column of the Periodic Table as Ti, is bulkier and slightly less electronegative.

The experiments in Ref. 13 were performed for a fixed Fe concentration (4 at. % Fe) and varying concentrations of Zr and Ti. The I_S were measured from 1 at. % Ti to 90 at. % Ti, in the β-Zr(Fe)-Ti alloys. For lower Ti concentrations it shows higher values (starting at -0.13 mm/s) than for pure β-Ti(Fe). The I_S decreases with increasing Ti concentration, until it reaches -0.22 mm/s, which corresponds to β-Ti(Fe) at 4 at. % Fe. The quadrupole splitting shows a very complex behavior, increasing from 0.24 mm/s (absolute value) at 1 at. % Ti to ~ 0.35 mm/s at 10 at. % Ti, then dropping to below 0.20 mm/s at 30 at. % Ti, and finally converging smoothly to the β-Ti(Fe) value at 4 at. % Fe (~ 0.20 mm/s).

Table V displays a series of results of calculations for Zr clusters, starting with Fe(Zr)$_{14}$ at distance 3.60 Å (corresponding to β-Zr). The I_S for this case can be extrapolated from the data in Ref. 13, and is less negative than for β-Ti(Fe). As is seen in Table V, for the lattice parameter of the host, the I_S does not compare well with experiment; therefore, as in the case of β-Ti(Fe), a local compression is predicted. For the corresponding host lattice parameters, the I_S calculated for β-Zr(Fe) is indeed higher than for β-Ti(Fe) by approximately the correct amount.

In Table V we also show the calculated value of ΔE_Q of the central Fe, produced by a Zr NN in the Ti host lattice, and two Zr NN (both of C_{3v} symmetry, at opposite sites with respect to the central Fe). In both cases, a negative field gradient is produced, which is more pronounced for the case of two Zr first neighbors. When, on the contrary, one Ti NN is in a Zr host, the field gradient produced on the central Fe atom is positive. This difference in the sign

of the Fe ΔE_Q produced by Ti or Zr at the same site may explain the complex behavior reported in Ref. 13 for the value of the ΔE_Q of β-Zr(Fe)-Ti for different Zr-Ti proportions in the host lattice.

In Table VI we separate the contributions to V_{zz} for the Fe-Ti-Zr clusters. The very small two- and three-center contributions again show that the NN Ti or Zr valence electrons are seen as point charges. The negative field gradient produced by one or two NN Zr atoms are due to the negative one-center contributions, whereas this contribution is positive when Ti is the NN atoms.

IV. CONCLUSIONS

We have performed electronic structure calculations for 15-atom clusters representing dilute bcc alloys of Fe in Ti, Zr, and the Ti-Zr system. The results show that local lattice compression will produce a small or null magnetic moment on Fe, and I_S values compatible with experiment. More concentrated alloys were represented by clusters in which the central Fe atom has another Fe atom in the first shell of neighbors, or in the second shell. The results for the calculated field gradients show that one Fe atom as NN or NNN produces a positive field gradient, due mainly to positive one-center contributions. Finally, studies of clusters representing the ternary alloys β-Zr(Fe)-Ti show that Zr or Ti as first-neighbor atoms produce field gradients with opposite signs on the Fe atom.

[1]A. D. McQuillan and M. K. McQuillan, *Titanium, Metallurgy of the Rarer Metals*, Vol. 4 (Butterworths, London, 1956).

[2]E. Galvão da Silva, *Investigation of Physical Properties of the Ti-Fe Alloy System Using Mössbauer Spectroscopy*, Saarlandes Universitat, Saarbrüken, West Germany, 1978 (unpublished).

[3]E. Galvão da Silva and U. Gonser, Acta Metall. 29, 903 (1981).

[4]E. Galvão da Silva and U. Gonser, Appl. Phys. A 27, 89 (1982).

[5]E. Galvão da Silva and U. Gonser (unpublished).

[6]M. M. Stupel, M. Ron, and B. Z. Weiss, J. Appl. Phys. 47, 6 (1976).

[7]G. Rupp, Z. Phys. 230, 265 (1970).

[8]C. Y. Yang, K. H. Johnson, D. R. Salahub, J. Kaspar, and R. P. Messmer, Phys. Rev. B 24, 5673 (1981), and references therein.

[9]J. Kaspar and D. R. Salahub, J. Phys. F 13, 311 (1983), and references therein.

[10]G. A. Benesh and D. E. Ellis, Phys. Rev. B 24, 1603 (1981).

[11]B. Delley, D. E. Ellis, and A. J. Freeman, J. Magn. Magn.

Mater. 30, 71 (1982).

[12]D. Guenzburger and D. E. Ellis (unpublished).

[13]E. Galvão da Silva, J. S. Coelho, and R. A. Mansur, Acta Metall. 30, 1829 (1982).

[14]D. E. Ellis, Int. J. Quantum Chem. S2, 35 (1968); D. E. Ellis and G. S. Painter, Phys. Rev. B 2, 2887 (1970).

[15]A. Rosén, D. E. Ellis, H. Adachi, and F. W. Averill, J. Chem. Phys. 85, 3629 (1976).

[16]J. C. Slater, *Quantum Theory of Molecules and Solids* (McGraw-Hill, New York, 1974), Vol. 4.

[17]R. S. Mulliken, J. Chem. Phys. 23, 1833 (1955).

[18]B. Delley and D. E. Ellis, J. Chem. Phys. 76, 1949 (1982).

[19]A. H. Stroud, *Approximate Calculation of Multiple Integrals* (Prentice-Hall, Englewood Cliffs, New Jersey, 1971).

[20]See, for example, N. N. Greenwood and T. C. Gibb, *Mössbauer Spectroscopy* (Chapman and Hall, London, 1971); J. M. Friedt and J. Danon, in *Modern Physics in Chemistry*, edited by E. Fluck and V. I. Goldanskii (Academic, London, 1979), Vol. 2; B. D. Dunlap and G. M. Kalvius, in *Mössbauer*

Isomer Shifts, edited by G. K. Shenoy and F. E. Wagner (North-Holland, Amsterdam, 1978).

[21]D. E. Ellis, D. Guenzburger, and H. B. Jansen, Phys. Rev. B **28**, 3697 (1983).

[22]D. Guenzburger and D. E. Ellis, Phys. Rev. B **22**, 4203 (1980).

[23]D. Raoux, A. Fontaine, P. Lagarde, and A. Sadoc, Phys. Rev. B **24**, 5547 (1981).

[24]D. Guenzburger, D. M. S. Esquivel, and J. Danon, Phys. Rev. **18**, 4561 (1978).

[25]W. C. Nieuwpoort, D. Post, and P. Th. Van Duijnen, Phys. Rev. B **17**, 91 (1978).

[26]E. V. Milczarek and W. P. Winfree, Phys. Rev. B **11**, 1026 (1975).